

COMPARISON OF POLARIZATIONS OF INCLUSIVELY PRODUCED
LAMBDA AND ANTILAMBDA BY PROTONS, ANTIPROTONS, KAONS AND PIONS ON HYDROGEN

A Proposal to Fermilab

by

M. A. Abolins (4), K. W. Edwards (3), W. R. Francis (5), S. Gourlay (1),
H. Kobrak (2) *, H. Melanson (4), D. P. Owen (4), R. E. Pitt (2),
R. A. Swanson (2) and P. M. Yager (1)

(1) University of California, Davis

(2) University of California, San Diego

(3) Carleton University

(4) Michigan State University

(5) Fermi National Accelerator Laboratory (Visiting Scientist)

*Correspondent

Physics Department (B-019)

University of California, San Diego

(714) 452-2291

INTRODUCTION

We propose to measure the polarization of lambdas (antilambdas) inclusively produced by protons, antiprotons, kaons and pions on liquid hydrogen.

Asymmetries will be measured to a statistical accuracy of $\delta a = 0.017-0.029$ ($\tilde{\delta}P = 0.027-0.046$) per t-bin in ten different t-bins for each reaction. These measurements will be done in a kinematic region where the asymmetry is expected to be as high as $a = 0.20$ ($P = 0.32$). We emphasize careful control of systematic effects on measured asymmetries by collecting simultaneously a large sample of $K_S \rightarrow \pi^+ + \pi^-$ decays.

This experiment, which was mentioned as part of our program in the proposal for E-383 and for which a letter of intent was submitted early in 1980, was prompted by the unexpectedly high lambda polarizations found first at Fermilab^{2,7,10} and later at the Cern PS⁶, the Brookhaven AGS⁸ and the CERN ISR⁴. At the 1980 Madison Conference some theoretical work on possible causes for this effect was reported⁹. Further details on these ideas are now available.³

The equipment to be used, as well as the analysis procedure, has been thoroughly tested in previous experiments (E-383, E-585) by the proponents. Only minimal changes to the equipment and the beam line are proposed. These changes are discussed in detail.

The cost to Fermilab is almost exclusively that of running the M-4 beam line and spectrometer.

We request approval to run for ten weeks at intensities and under beam conditions which are discussed in detail. The running is proposed to follow immediately the completion of the data collection for E-585.

predictions of QCD. Figure 1 illustrates the essential character of the QCD predictions for scale violation in the nucleon structure functions as Q^2 is increased. There are relatively large violations at small values of Q^2 ($1 < Q^2 < 10 \text{ GeV}^2$) and small violations at large Q^2 ($Q^2 > 100 \text{ GeV}^2$).

With no other information at hand, it would seem obvious that the most critical measurements could be made in the range $1 < Q^2 < 50 \text{ GeV}^2$; indeed, this was the prevailing view during the decade of the 1970's. After an initial euphoria induced by a less than critical comparison of low Q^2 data with first order QCD predictions¹, two theoretical observations cooled the general ardor: i) Haim Harari demonstrated that the general features of scale violations could be obtained by many field theory models² and were by no means exclusive to QCD; ii) the emergence of second order QCD calculations and estimates of higher order effects³. The so-called "higher twist" effects⁴, seem to put a lower limit on the Q^2 range where reliable comparisons can be made between QCD and experimental results. Since the numerical predictions of QCD rely on perturbation methods, and since the effective expansion parameter is $1/\ln(Q^2)$, it is clear that measurements must extend to Q^2 values very much higher than 20 GeV^2 to be useful for comparison with theory.

But here again there is a problem. Even if extreme center of mass collision energies are possible (ep colliders), three things conspire to limit the power of a QCD test: i) the scale violation effect varies as a logarithm; ii) the integrated

number of events, hence the statistical power of the test, drops as $1/Q^2$, making luminosity requirements more severe as the Q^2 scale rises; iii) the ordinary QED radiative corrections become extremely large for ep collider energies. While calculable in principle, these large corrections must influence the reliability of observing the much smaller QCD effects one is attempting to measure.

With Tevatron energy muon beams, the useful Q^2 range experimentally accessible is broad enough to investigate these QCD effects, and radiative corrections are not a problem. However, we are faced with the question of target and method. The natural targets are hydrogen and deuterium, but these must be exceptionally long (tens of meters) to reach the highest Q^2 values with useful statistics. If such targets are used, vertex location, hence Q^2 resolution, may be compromised resulting in unacceptable systematic errors at low values of Q^2 . On the other hand, sufficient luminosity can be obtained with solid targets of a modest length. The drawbacks of nuclear targets, particularly those with large atomic number, are the theoretical uncertainties in the interpretation of the results. First, it is difficult to extract structure functions of individual nucleons. Second, there are the problems that arise from Fermi motion in the nuclei and from real radiative corrections and nuclear shadowing effects.

We choose a two part program that accomplishes a large part of the structure function program in a way that is com-

patible with the study of recoil hadrons from thin nuclear targets. Phase I of the structure function measurements would be undertaken with 2.7 meter segmented Be target. The results from this experiment will give general guidance for the hydrogen/deuterium runs to follow as well as a first look at the structure functions above $Q^2 = 200 \text{ GeV}^2$. If theory continues to progress in the intervening period, the Be results may themselves be useful for QCD comparisons, but the primary motivation will be to survey the high Q^2 terrain with good Q^2 resolution. Following the Be running and further hadron studies with a vertex detector, a series of runs would be undertaken using a 10 meter hydrogen/deuterium target (Phase III of this proposal). The hydrogen/deuterium running would be used for a high resolution, good statistics study of structure functions in the low and intermediate Q^2 regime, $2 < Q^2 < 400 \text{ GeV}^2$. We expect to be able to extract the essential QCD test results from this data range, and leave the small, but difficult, region of high y and Q^2 to more specialized experiments.

B. Hadron Production in Muon-Nuclear Scattering

One of the central problems in the quark model of hadron structure is why a quark, when struck by a lepton or some current, is not seen to emerge as a free particle. If the quarks are confined to within the hadron the question then centers upon the dynamics of the confinement process and the closely associated question of the evolution of multiparticle states after the excitation of quarks in an elementary particle collision.

An important technique that is available for directly observing the development of the final state is the use of collisions on nuclei. The idea behind this technique is straightforward: in order to directly study the evolution of a state it is necessary to interfere with it while it is evolving. The distances involved in particle production at high energies are such that a large nucleus can effectively play the role of the production target followed by an "interfering system".

The study of hadron-nucleus collisions has already given a number of surprises and considerable insight into the space-time development of the production process.⁵ Unfortunately, because of the compound nature of the incident state and therefore inherent complexity of the initial interaction, a detailed interpretation of the data is difficult. On the other hand, there is good reason to believe that the interpretation of deep inelastic, lepton-nucleus collisions is more straightforward and as a consequence that such studies will give invaluable information on the dynamics of quark fragmentation into hadrons.⁶

From a naive quark-parton viewpoint the picture of inelastic lepton scattering off nucleons can be described as follows.⁷ A virtual photon is emitted by the lepton in its passage through or near a nucleon. For small values of Bjorken x ($\lesssim 0.1$), the photon has time to produce virtual $q\bar{q}$ pairs before interacting with the nucleon. The photon's interaction

is thus hadron-like. For larger x the photon is absorbed by a constituent quark in the nucleon. The struck quark receives an energy ν and attempts to leave the nucleon, but because of the confining forces, it fragments instead into a jet of particles. This fragmentation process takes place over a distance of the order of ν/m^2 , where $m \approx 1$ GeV.

An alternative viewpoint is that Q^2 and not x is the relevant parameter for separating the hadron-like and point-like regions of the virtual photon.⁸ In this case, the virtual photon interaction with a quark can be considered point-like for $Q^2 \gtrsim 1$ GeV². Our experiment will determine whether crossing a Q^2 threshold is a sufficient condition for observing the effects of individual quarks.

In either case the scattered lepton effectively tags the hadron jet which is produced in, and passes through, the nuclear matter. For low values of x , or Q^2 , the A -dependence of the produced hadrons should be similar to that in hadron-nucleus collisions at an incident energy of ν GeV. This will be an interesting check on our understanding of the process taking place but will probably not contain information which cannot be obtained from hadron-nucleus collisions. However, in the region of pointlike scattering, the variation with ν of the A -dependence of the produced particles should prove fascinating.

Figure 2 summarizes the relation between x , ν , and Q^2 and the various distances of interest in this experiment. The

important measurements to be made in such an experiment and their interpretation are as follows:

1) The variation with A of the multiplicity and of the longitudinal rapidity distribution in the direction of the virtual photon gives information on the time structure of the quark hadronization process.

2) A measurement of the attenuation of the leading hadrons as a function of nuclear thickness gives information on the absorption of fast quarks by nucleons. Furthermore, the difference between π and K attenuation is related to the difference between the absorption cross sections of strange and non-strange quarks.

3) For similar reasons, the A -dependence of the width of the p_{\perp} distribution of leading hadrons about the direction of the virtual photon gives information on the differential cross section of quarks on nucleons.

Several authors have made predictions of what one might expect to see. Their models for quark fragmentation estimate that hadrons of energy E are formed after a time E/m^2 , where m^2 is of order 2 GeV^2 . Thus the multiplicity of high energy hadrons should be independent of the nuclear mass number A except for secondary interactions of the emerging quark. Bialas and Bialas⁹ have made estimates for two observable effects of such interactions. The first is a depletion of high energy hadrons as A increases because of inelastic interactions of the quark. Figure 3 shows the expected depletion as a function of A for

reasonable choices of the quark-nucleon absorption cross section. The quantity R is the ratio of hadron multiplicity with a nuclear target to that with a hydrogen target. The second effect is a broadening of the distribution dN/dp_{\perp}^2 of high energy hadrons due to multiple elastic scattering of the emerging quark. Figure 4 shows the results of the Bialas model.

Hadrons of lower energy than the above are formed inside nuclear matter; they undergo nuclear cascading, which has the effect of depleting the spectrum for high energies and enhancing the multiplicity at low energies. Hadrons formed outside the nucleus do not contribute to this process; the result is a drop in multiplicity which is clearly seen in the calculation of Davidenko and Nikolaev¹⁰ shown in Figure 5. Here R is plotted as a function of hadron momentum k . The interpretation of these curves is relatively straight-forward. The highest momentum hadrons are formed outside the nucleus. Their multiplicity is independent of nuclear size, and the threshold k_T , above which $R = 1$, increases linearly with nuclear radius, but does not depend on quark energy v . Hadrons with momentum k just below k_T are depleted by nuclear cascading; this produces a dip in R around 8-30 GeV/c and an increase in R below 5 GeV/c from the cascade products. This dip is characteristic of the class of models using short range correlation. Models emphasizing the production of hadrons through color neutralization, as advocated by Brodsky⁸, predict instead that R smoothly

interpolates between the target and beam fragmentation regions. We should be able to resolve this issue, hopefully gaining insight into the quark fragmentation process and the interaction of quarks with nuclear matter.

C. Hadron Jets in Muon-Nucleon Scattering

1. General

The importance of measuring the hadronic final state in lepton-nucleon interactions is that it provides a clearly prepared excited baryon. Unlike e^+e^- jets, the axis of the jet is measured by the scattering of the lepton and thus deviations from their low Q^2 behavior can be measured with respect to a well-defined frame. Gluon radiation and Q^2 -dependent meson distributions can be picked up more easily given this frame of reference.

A further merit of muon scattering, if both proton and deuterium targets are used, is that it allows measurement of all the functions used to describe the collision and subsequent meson production. One can measure not only the valence and sea quark structure functions, but also the quark fragmentation functions, $D(x_F)$. These measurements become more important with the advent of QCD where one expects non-scaling deviations in all of these quantities dependent on Q^2 . There exist measurements of muon-produced hadrons at 150 GeV incident energy¹¹; however, these data are limited to very forward hadrons, $x_F > 0.2$.

2. Gluon Jets?

One of the most fruitful uses of μ -meson scattering is a "clean" test for gluon radiation effects.¹² There appear to be such effects in high energy hadron final states from e^+e^- annihilation. However, these three jet structures can also arise from other models, such as a two jet model, when planar events are selected.¹³ In the case of lepton scattering the jet axis and the $\phi=0$ origin for measuring cylindrical asymmetries are determined by the virtual photon direction, which is independent of any knowledge of the hadronic final states. Furthermore, the quark jet from protons is dominated by a leading u-quark giving rise to π^+/π^- ratios as high as 2.5 at high x_F and Q^2 . We then have the possibility of statistically separating the quark jet and the gluon jet.

The ϕ distribution of hadrons about the jet axis in the high x_F range may be written as $a + b \cos\phi + c \cos^2\phi$. Georgi and Politzer¹² have calculated a typical value of b and find that it can be as large as $-0.24a$ at high energies (200 GeV). J. Cleymans¹⁴ has derived an expression for c and finds it comparable with b . The b and c terms are of order $\alpha_s a$ (α_s is the quark-gluon coupling constant).

The ϕ distribution has been measured at low energies¹⁵ and at Fermilab¹⁶, and no asymmetry was observed. However, the acceptance corrections to the ϕ distribution were large in these experiments, which demonstrates the need for an apparatus with uniform ϕ acceptance.

3. Charge and Baryon Number Distributions

The so-called leading charge effect is well known; it is presumably an indication of the u or d character of the forward quark. In e or μ -hadron scattering, it is positive due to the larger charge of the u-quark and its predominance in protons. It has been speculated that the average charge of the forward jet would be related to the struck quark charge both in e or μ and neutrino events.¹⁷ Experimental measurements claim to confirm this expectation¹⁸, but in all cases the charge was measured by looking at all hadrons. The yields for mesons alone are shown in Figure 6 from an experiment which separated mesons from protons.¹⁵ The net charge carried by the meson cloud for $x_F > 0$ is ~ 0.2 . If one looks at all hadrons with apparent $x_F > 0$ the net charge increases to ~ 0.6 . The discrepancy is accounted for by protons with $x_F \lesssim 0$, whose calculated x_F when treated as π -mesons is positive.

Two experiments¹⁹ have investigated the distribution of residual protons in e-proton scattering; this is defined as the yield of protons minus anti-protons and thus indicates the distribution of the baryonic charge. These experiments suggest that there are two groupings of protons: one with x_F near -1.0 and the other with $x_F \simeq -0.2$ (see Figure 7). The relative yield of the latter increases with x_{Bj} , suggesting that it might be connected with interactions involving valence quarks. It is these protons which contaminate the π^+ meson cloud in the forward direction. It also appears that \bar{x}_F for these protons

increases with energy.

In order to further investigate these phenomena it will be necessary to have a muon spectrometer plus a vertex detector with full x_F and ϕ acceptance. Ultimately, it will also be important for the device to be able to separate low momentum pions and protons.

III. Proposed Experimental Program

A. Overview

We propose a three-phase program of muon scattering studies at the Tevatron. The initial phase will require a rebuilt version of the Cyclotron Magnet Spectrometer and will include measurements of inclusive muons from a 3m long Be target as well as studies of the forward hadrons produced from thin nuclear targets. The second phase will include a magnetic vertex detector to study hadron production at all angles from thin nuclear and H_2/D_2 targets. In the final phase, long H_2/D_2 targets will be used for structure function studies and QCD tests.

B. Phase I

The purpose of this phase of the experiment is threefold. First we will explore the new Q^2 range opened up by the higher Tevatron energies. Second, we will take a first look at the high momentum hadrons which are within the acceptance of the Cyclotron magnet. And finally, we will be doing the shakedown experiment with an essentially new muon spectrometer.

For Phase I we propose to run for 1000 hrs. with a 600 GeV/c muon beam accumulating a total of 2.2×10^{12} muons. As shown in Table I, this assumes a muon yield of $5 \cdot 10^{-6}$ per incident proton for the Tevatron muon beam, and $7 \cdot 10^{12}$ protons per spill. The inclusive muon yields for this run with a 3m Be target are given in Table II.

For the hadron studies in Phase I we will use thin, solid targets of C, Cu, and Pb, and a 50 cm liquid deuterium target.

These targets will be sequentially placed at the edge of the uniform field region for the Cyclotron magnet (see Figure 10) to maximize the acceptance. The size of the targets and the running time spent on each are given in Table IV along with corresponding number of events obtained. The distribution of the high momentum hadrons for these events, as predicted by the Field-Feynman model²⁰, is shown in Table V.

Because of the need to minimize electromagnetic pair production and secondary hadron scatters, we will use several thin (10% radiation length) targets dispersed along the beam. The Pb and Cu targets will both be segmented into four foils, each approximately 10% of a radiation length thick and separated by 2 cm gaps. A 40% radiation length C target is already 10 cm long and sufficiently dispersed, as is the D₂ target. The vertex position of an event within the target will be determined to ± 1 cm by the reconstruction of outgoing tracks with lab angles greater than 100 mrad. We can then bin the events according to how much target material is traversed by the secondary tracks. An extrapolation to zero target thickness will correct for π^0 conversions, hadron rescatters, etc. For high momentum hadrons where statistics are sparse, but multiplicative effects are small, it should be possible to treat the target as a single entity.

C. Phase II

For Phase II we will have installed a magnetic vertex detector as described in Section IVB and shown in Figure 11. We then

propose to run for another 1500 hrs. at 600 GeV/c to study the muon-produced hadrons in greater detail and with much improved acceptance. The uniformity of the magnetic field in the vertex detector will allow us to use two nuclear targets simultaneously, separated by 1 m., and a deuterium target which is twice as long (1m). Thus for 1000 hrs. of running, target doubling increases Phase I event yields shown in Table IV by a factor of two. An extra 500 hrs. will then be spent with a 1 m liquid hydrogen target, yielding approximately the same number of hydrogen and deuterium-produced events.

D. Phase III

In Phase III the vertex detector would be replaced by a 10 m. long liquid hydrogen/deuterium target. 2000 hrs. of running would then be required for an investigation of nucleon structure functions and QCD testing. The time would be evenly split between hydrogen and deuterium giving the event yields shown in Table III.

IV. Apparatus

A. Cyclotron Magnet Spectrometer (Phase I)

A schematic drawing of the proposed open geometry muon spectrometer is shown in Figure 8. This spectrometer is a modernized version of the CCM spectrometer that was used for E98 and subsequent experiments in the old muon laboratory.²¹ The cyclotron magnet itself is currently being outfitted with superconducting coils, and therefore will be an ideal centerpiece of a Tevatron era magnetic spectrometer.

The location of the high luminosity Be and H_2/D_2 targets for Phases I and III respectively are shown in the figure. The Phase II vertex detector will occupy approximately the same location as the Phase I Be target. The scattered muon acceptance function for both of these target locations is shown as a function of y and Q^2 in Fig. 9·abc. The acceptance deviates from unity only in the region of high Q^2 and high y . For Phase I the thin foil targets are placed at the upstream edge of the magnet pole for two reasons. First, this optimizes the acceptance for forward hadrons. Second, for ease of analysis it is desirable to have the targets followed by a region of nearly uniform magnetic field. This is seen to be the case from the plot of the radial variation of the field in Fig. 10.

The 10 planes of MWPC that follow both the high luminosity targets and the thin foil targets are already in existence and are being used in experiment E610. However, the two downstream drift chamber modules would be new for this experiment. Both

of the packages would contain four pairs of drift planes with 5 cm cell width. Each wire would be read out by electronics with multi-hit capability.

An event will be signalled by a particle traversing the downstream Fe Absorber and firing one element of the trigger counter array. An event will be vetoed if there is a count in the upstream halo veto wall or in the downstream beam veto counter.

The estimated cost of reinstrumenting the spectrometer is summarized below.

Two Drift Chamber Modules

Electronics	\$250 K
Materials and assembly	50 K
<u>Trigger Counters and Misc.</u>	100 K
<u>Electronics</u>	<u>200 K</u>
	\$600 K TOTAL

B. Vertex Detector (Phase II)

A detailed study of leptoproduced hadrons will require full coverage of the events produced in μ scattering. However, a single, high field magnet is not adept at covering the very large range in momenta: the inelastically-scattered μ requires a high $B\ell$ for accurate measurement, yet nearly half the emerging particles are in the momentum range of 1 GeV/c or below. Though in principle it is possible to reconstruct a track of low momen-

turn and therefore small radius of curvature, in practice this is difficult without human scanning. We have done a study of automatic computer track reconstruction of high energy μ events. We find that track recognition begins dropping from 100% efficiency for radii of curvature of about 3 meters in a realistic multichamber detector in a magnetic field.

We therefore propose to place the Phase II targets in the low field vertex detector magnet, shown in Figure 11. In order to achieve reasonable luminosity we require at least a one meter long H_2/D_2 target; we would also like to have a pair of thin nuclear targets separated by about a meter. These requirements set the scale of the magnet at 2.5 m long by 1.5 m wide by 1 m. high. The magnet would be filled with planar MWPC's which surround the targets. The field would be low, 1.5 kgauss, corresponding to a radius of curvature of 45 m and a minimum sagitta of $\sim 3\text{mm}$ for a 2 GeV/c track. Higher momentum tracks would be measured in the field of the cyclotron magnet.

The proposed vertex detector magnet will be relatively inexpensive to build; because of its low field it requires less than 10 tons of steel for the return yoke. In addition it can be wound with conventional coils and will draw less than 150 k watts of power. The MWPC packages shown in Figure 11 will have large groups of wires read out by charge division techniques. For a given cost this will maximize the total number of wires available for track reconstruction.

Thus, for a modest investment, we will be able to construct

a vertex detector capable of measuring hadronic secondaries to momenta as low as 200 MeV/c. This would satisfy most of the physics goals outlined in Section II. We are also considering more elaborate vertex detectors, which would allow us to separate low-momentum pions and protons, in addition to measuring their trajectories.

REFERENCES

1. H.L. Anderson et al., Phys. Rev. Lett. 40, 1061 (1978);
J.G.H. de Groot et al., Phys. Lett. 82B, 292 (1979).
2. H. Harari, Nucl. Phys. B161, 55 (1979).
3. W.A. Bardeen et al., Phys. Rev. D18, 3998 (1978).
4. M. Barnett, SLAC-Pub-2396 (1979).
5. W. Busza, Acta Phys. Polon. B8, 333 (1977).
6. J.D. Bjorken, SLAC-Pub-1756 (1976).
7. V.N. Gribov, JETP 30, 709 (1970).
8. S.J. Brodsky, SLAC-Pub-2395 (1979).
9. A. Bialas and E. Bialas, FERMILAB-Pub-79/57.
10. G.V. Davidenko and N.N. Nikolaev, Nucl. Phys. B135, 333 (1978).
11. W.A. Loomis et al., Phys. Rev. D19, 2543 (1979).
12. H. Georgi and H. David Politzer, Phys. Rev. Lett. 40, 3 (1978).
13. D.P. Barber et al., Phys. Rev. Lett. 43, 830 (1979).
14. J. Cleymans, University of Bielefeld Preprint BI-TP T8/02 (1978).
15. J.F. Martin et al., Phys. Rev. D20, 5 (1979).
16. C. Tao, Harvard Ph.D. Thesis (1980).
17. R.P. Feynman, Neutrino Conference, Balaton, Hungary (1972).
18. N. Schmitz, Lepton-Photon Conference, Fermilab (1979).
19. C.J. Bebek et al., Phys. Rev. Lett. 34, 1115 (1975);
L.S. Osborne et al., Phys. Rev. Lett. 41, 76 (1978).
20. R.D. Field and R.P. Feynman, CALT-68-618 (1978).
21. B.A. Gordon et al., Phys. Rev. D20, 2645 (1979).
22. J.G.H. de Groot et al., Phys. Lett. 82B, 456 (1979).

TABLE I

Muon Flux and Event Rates

<u>Muon Energy</u>	<u>Yield</u> (μ /incident p)	<u>Time*</u> (hr/ $10^{12} \mu$)	<u>Spill Rate*</u> (μ /sec)	<u>Events/10^{12}/gm/cm²</u>		
				$Q^2 > 1$	$Q^2 > 5$	$Q^2 > 50$
450	$4 \cdot 10^{-5}$	60	$2 \cdot 8 \cdot 10^7$	275 K	29 K	450
600	$5 \cdot 10^{-6}$	450	$3 \cdot 5 \cdot 10^6$	300 K	33 K	650
750	$4 \cdot 10^{-7}$	6000	$2 \cdot 8 \cdot 10^5$	320 K	37 K	820

*Assuming $7 \cdot 10^{12}$ incident protons/spill and one 10 sec spill/minute.

TABLE II

MUON NUCLEON SCATTERING
EVENT YIELDS

TGT = 2.7 M Be
 FLUX = 2.2×10^{12} MUONS
 TIME = 1000 HOURS
 $E_{\mu} = 600$ GeV
 $E_p = 800$ GeV

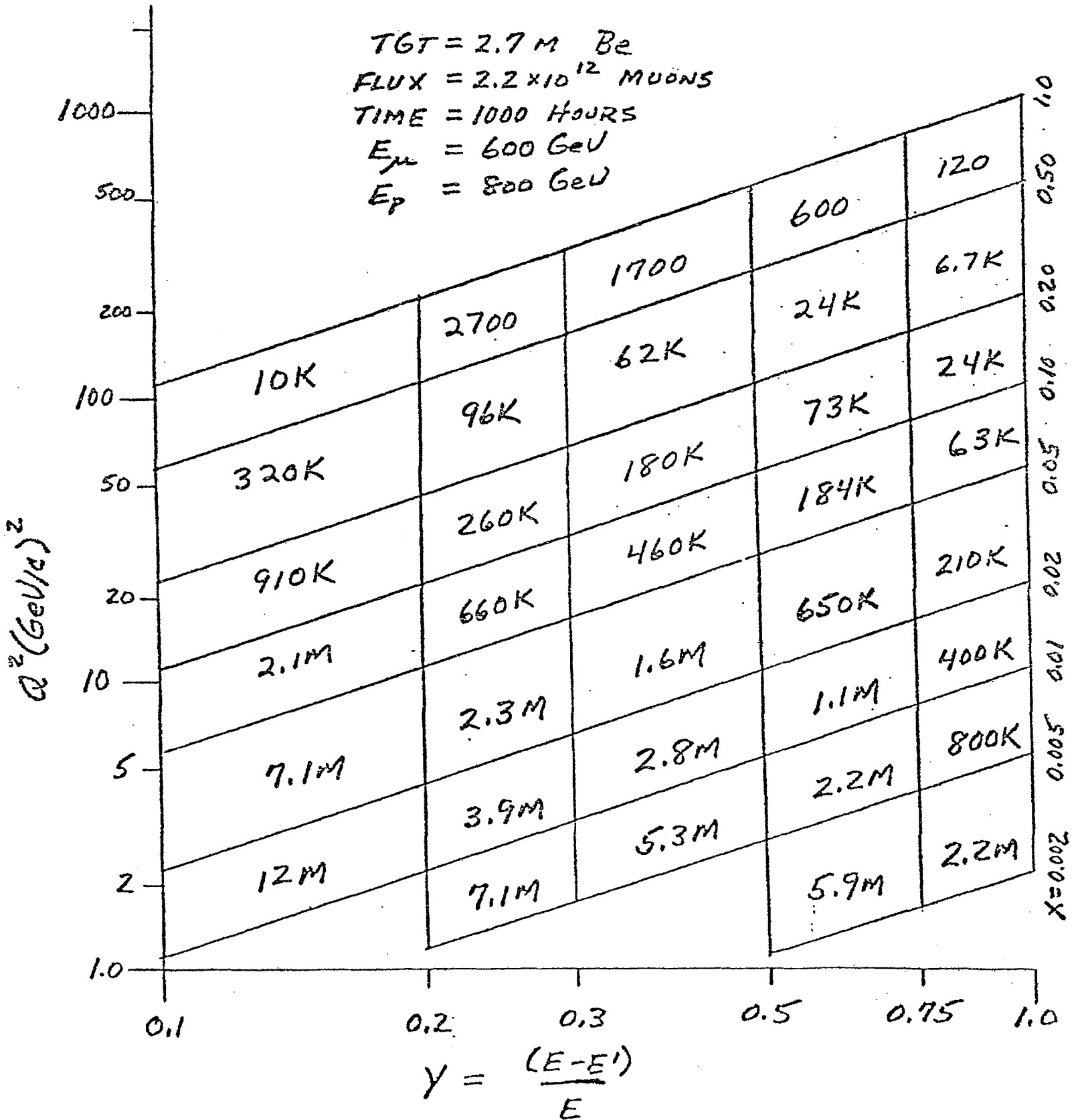
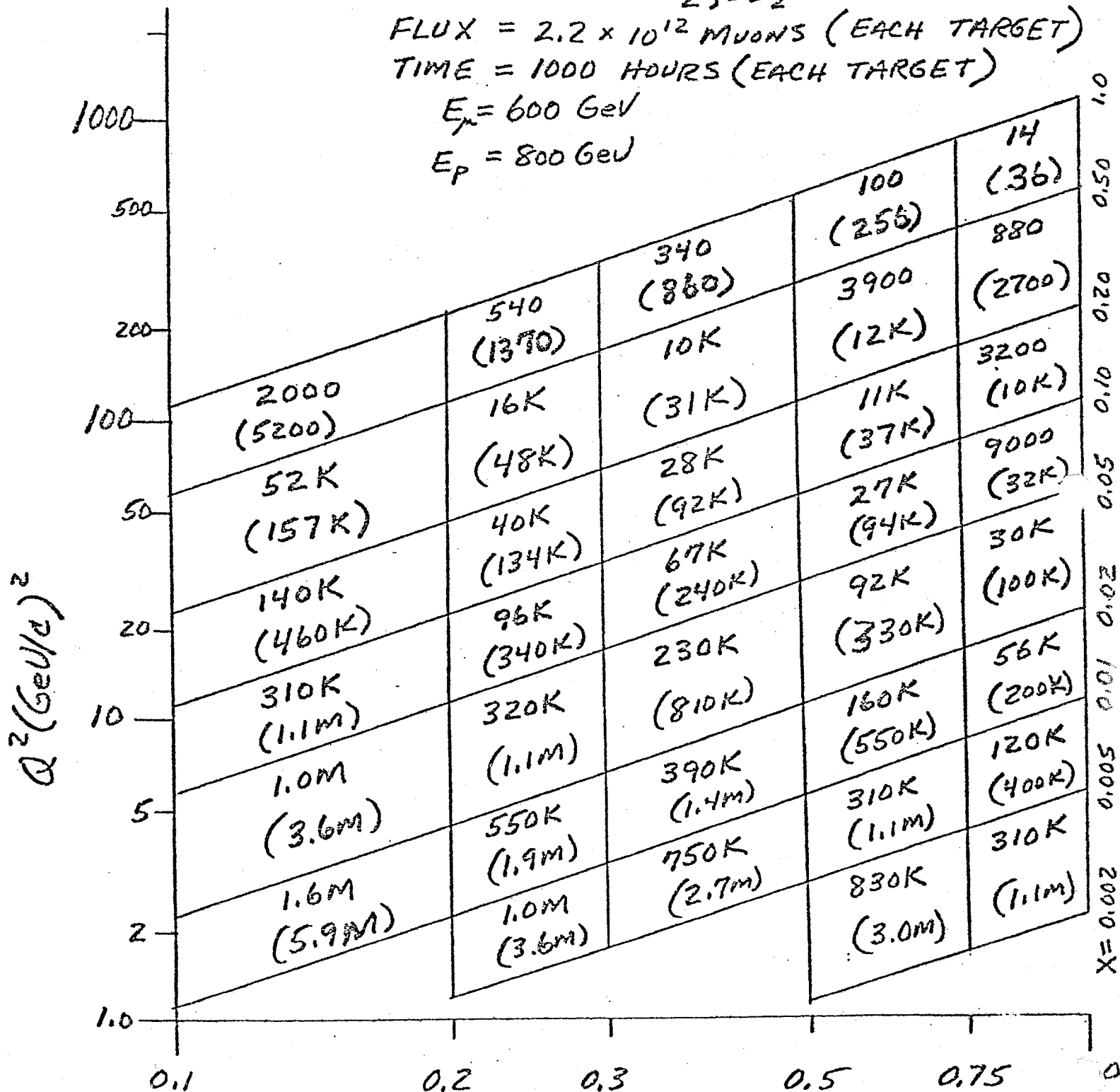


TABLE III

MUON NUCLEON SCATTERING
EVENT YIELDS

TGT = 10 M LH₂, LD₂*
 FLUX = 2.2 x 10¹² MUONS (EACH TARGET)
 TIME = 1000 HOURS (EACH TARGET)
 E_μ = 600 GeV
 E_p = 800 GeV



* LD₂ YIELDS
IN PARENTHESES

$$y = \frac{E - E'}{E}$$

TABLE IV

Thin Target Program - 600 GeV Muons

<u>Target</u>	<u>Length</u> (gm/cm ²)	<u>Run</u> (Hrs.)	<u>Total</u> <u>Muons</u>	<u>Q² > 1 GeV²</u>	<u>Events</u> <u>> 5 GeV²</u>	<u>> 50 GeV²</u>
C	4 x 4.3	100	2x10 ¹¹	1.2 x 10 ⁶	1.3 x 10 ⁵	2400
Cu	4 x 1.3	300	7x10 ¹¹	1.0 x 10 ⁶	1.2 x 10 ⁵	2200
Pb	4 x 0.7	400	9x10 ¹¹	0.8 x 10 ⁶	0.8 x 10 ⁵	1600
D ₂	8.2	200	4x10 ¹¹	1.1 x 10 ⁶	1.2 x 10 ⁵	2300

TABLE V

Hadron Momentum Distributions - 600 GeV Muons

<u>Hadron Momentum</u> (GeV/c)	<u>Hadrons / 1000 Events</u>	
	<u>$Q^2 > 1 \text{ GeV}^2$</u>	<u>$Q^2 > 5 \text{ GeV}^2$</u>
10 < p < 50	800	1200
50 < p < 100	110	180
100 < p < 200	40	60
200 < p < 400	6	9
p > 50, p _⊥ > 1	6	9

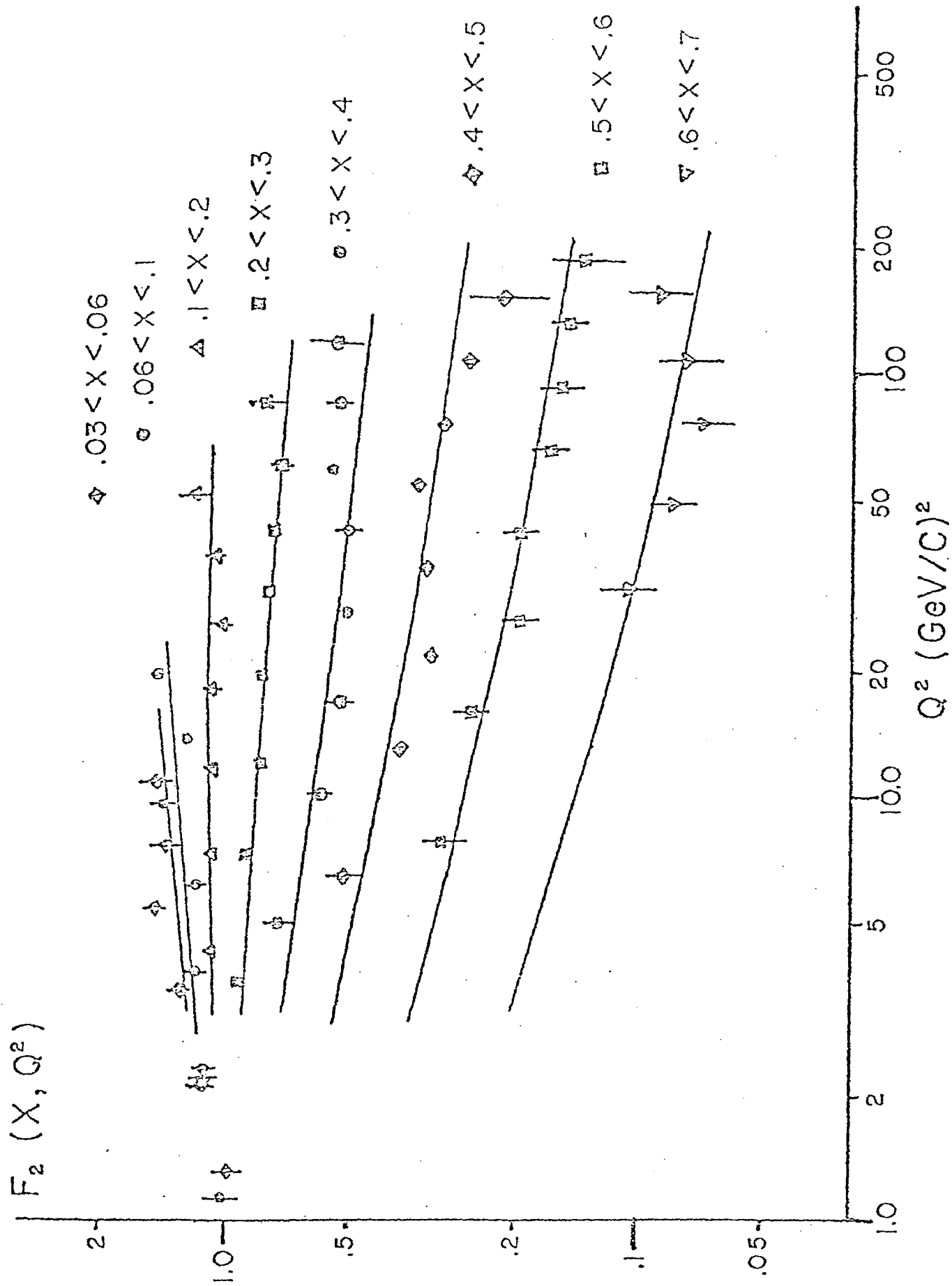


FIG. 1 (Ref. 22)

ORDER OF MAGNITUDE OF DISTANCE IN
LAB OVER WHICH QUARK FRAGMENTS INTO HADRONS

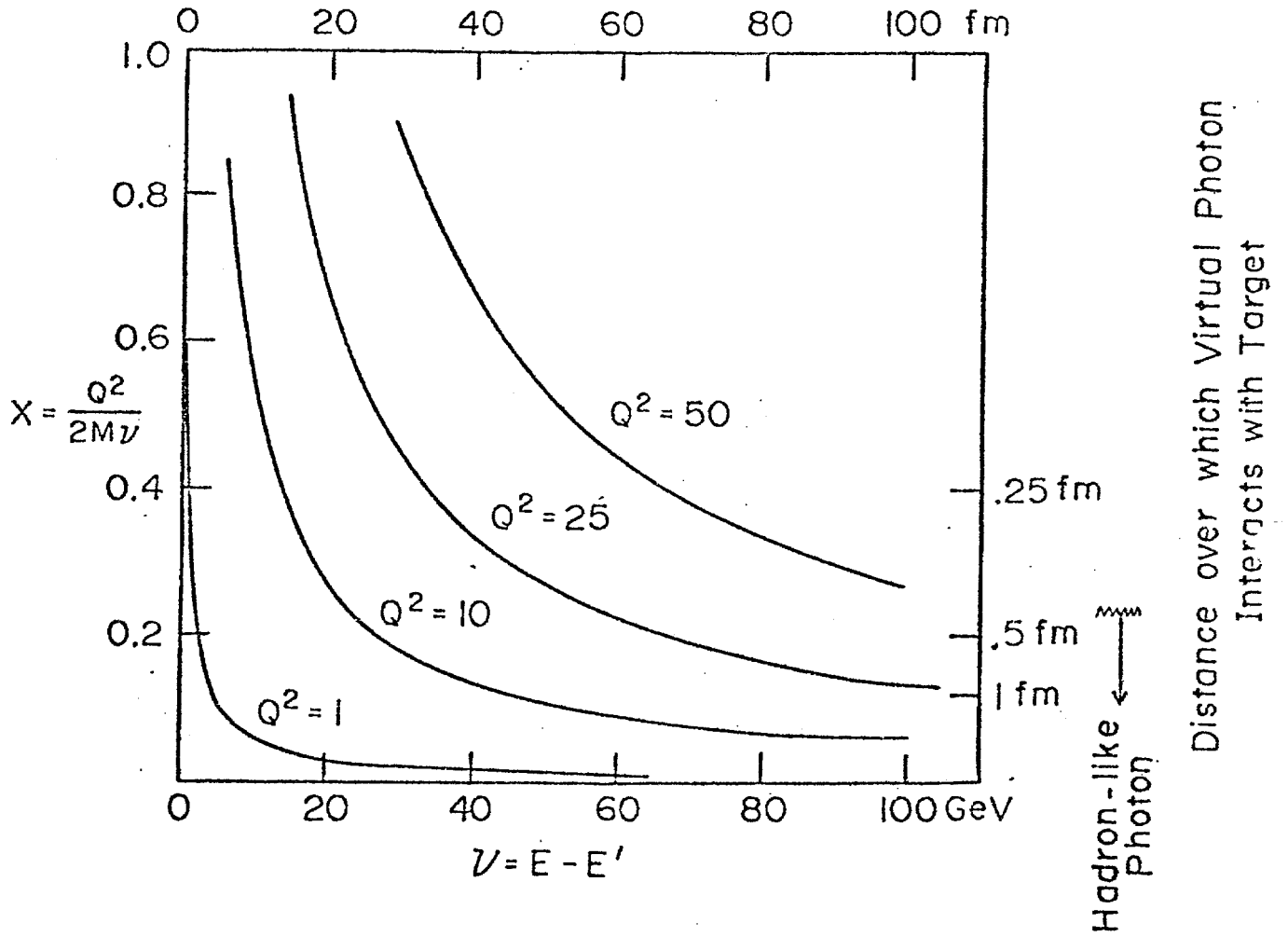


FIG. 2

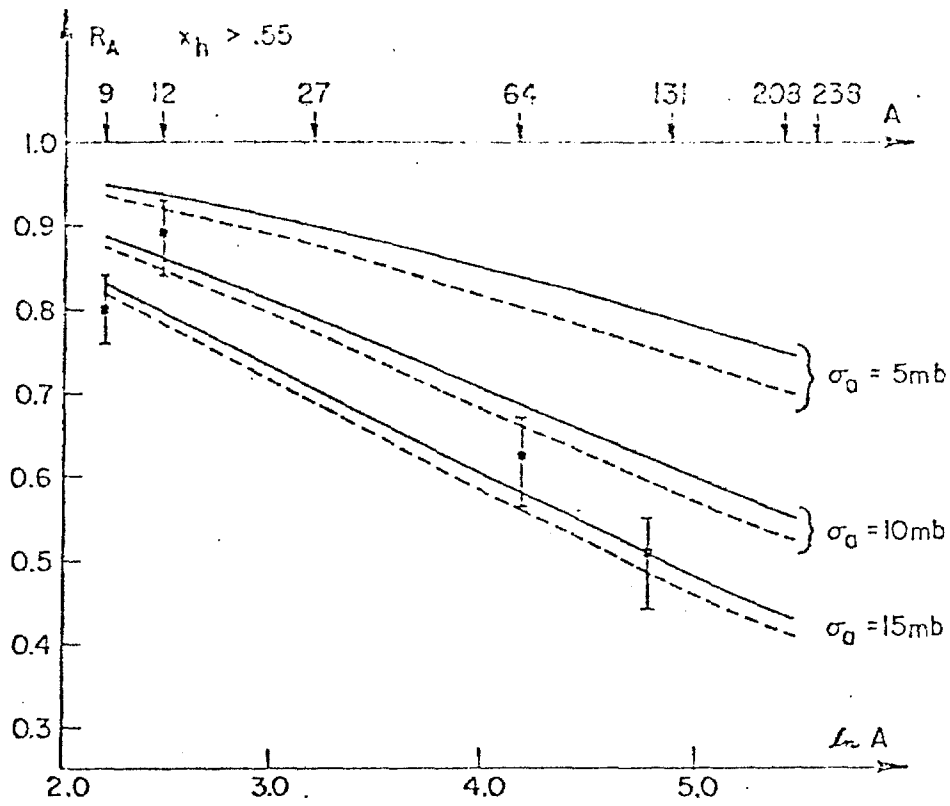


FIG. 3 (Ref. 9)

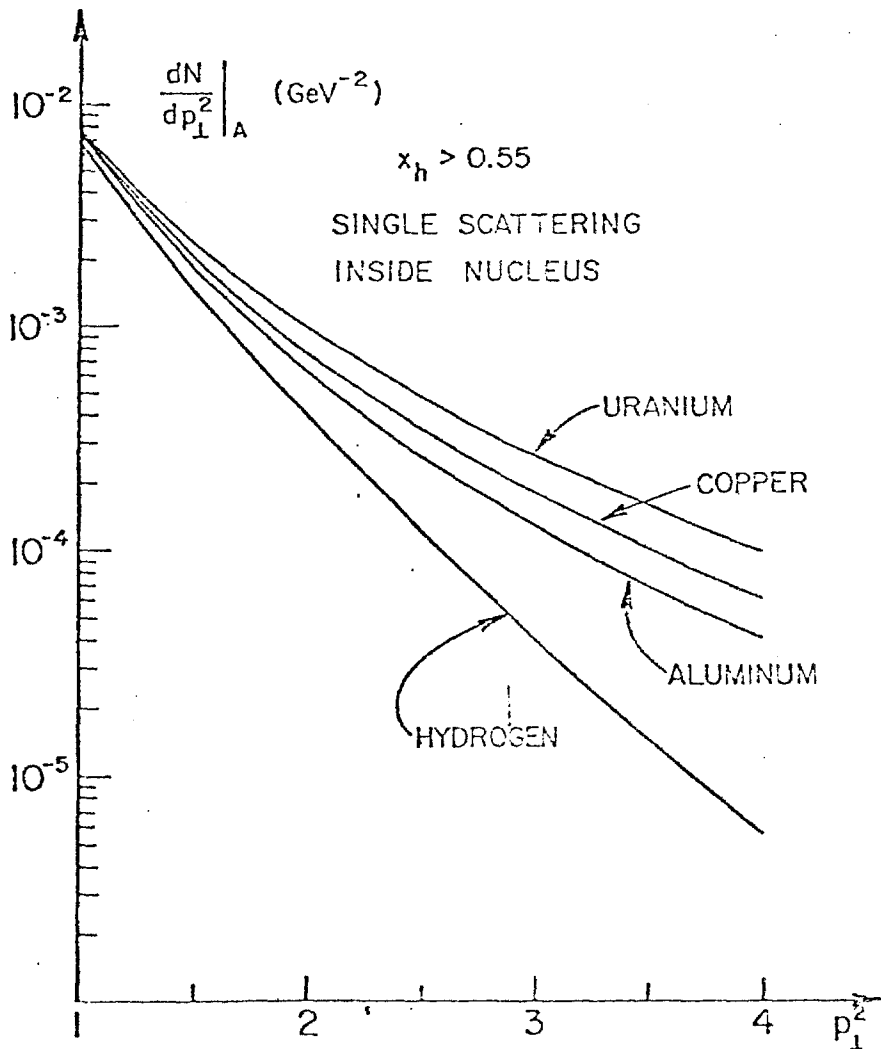


FIG. 4 (Ref. 9)

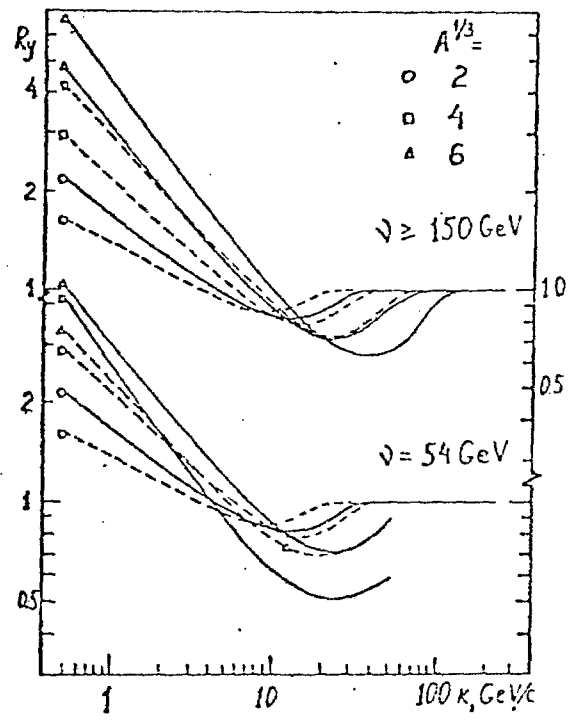


FIG. 5 (Ref. 10)

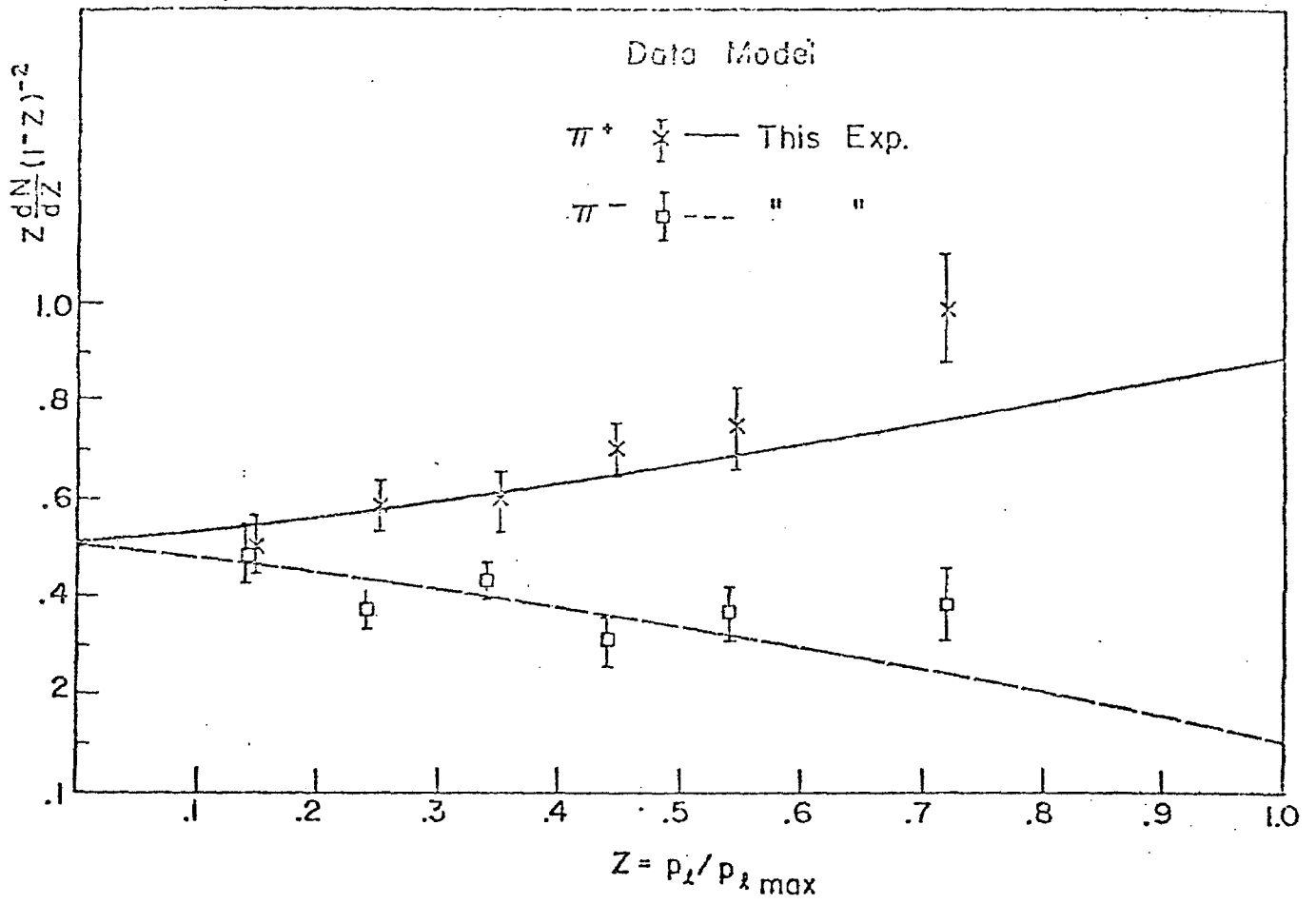


FIG. 6 (Ref. 15)

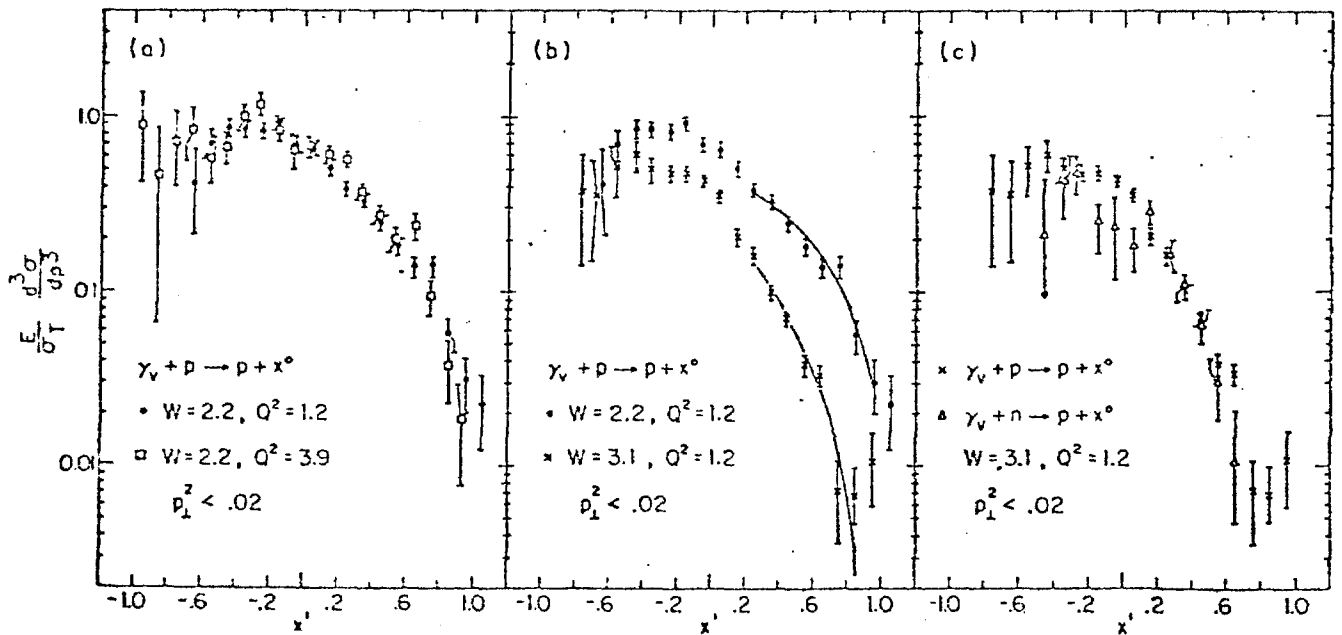
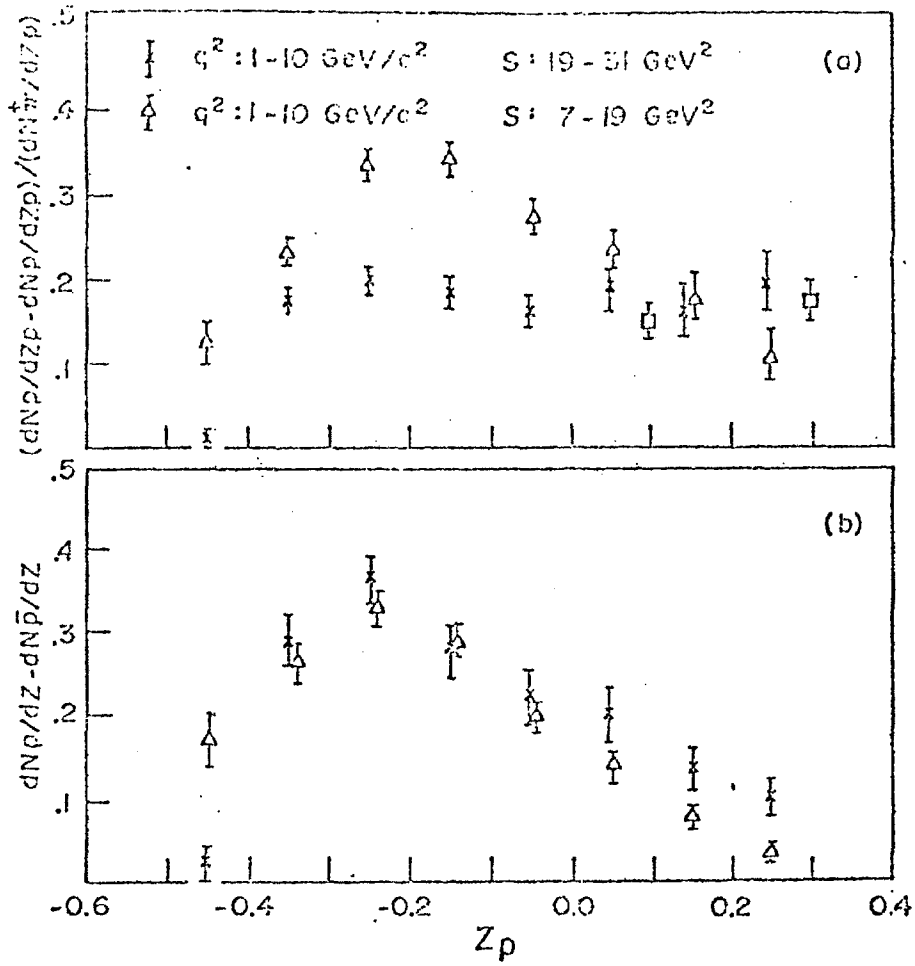
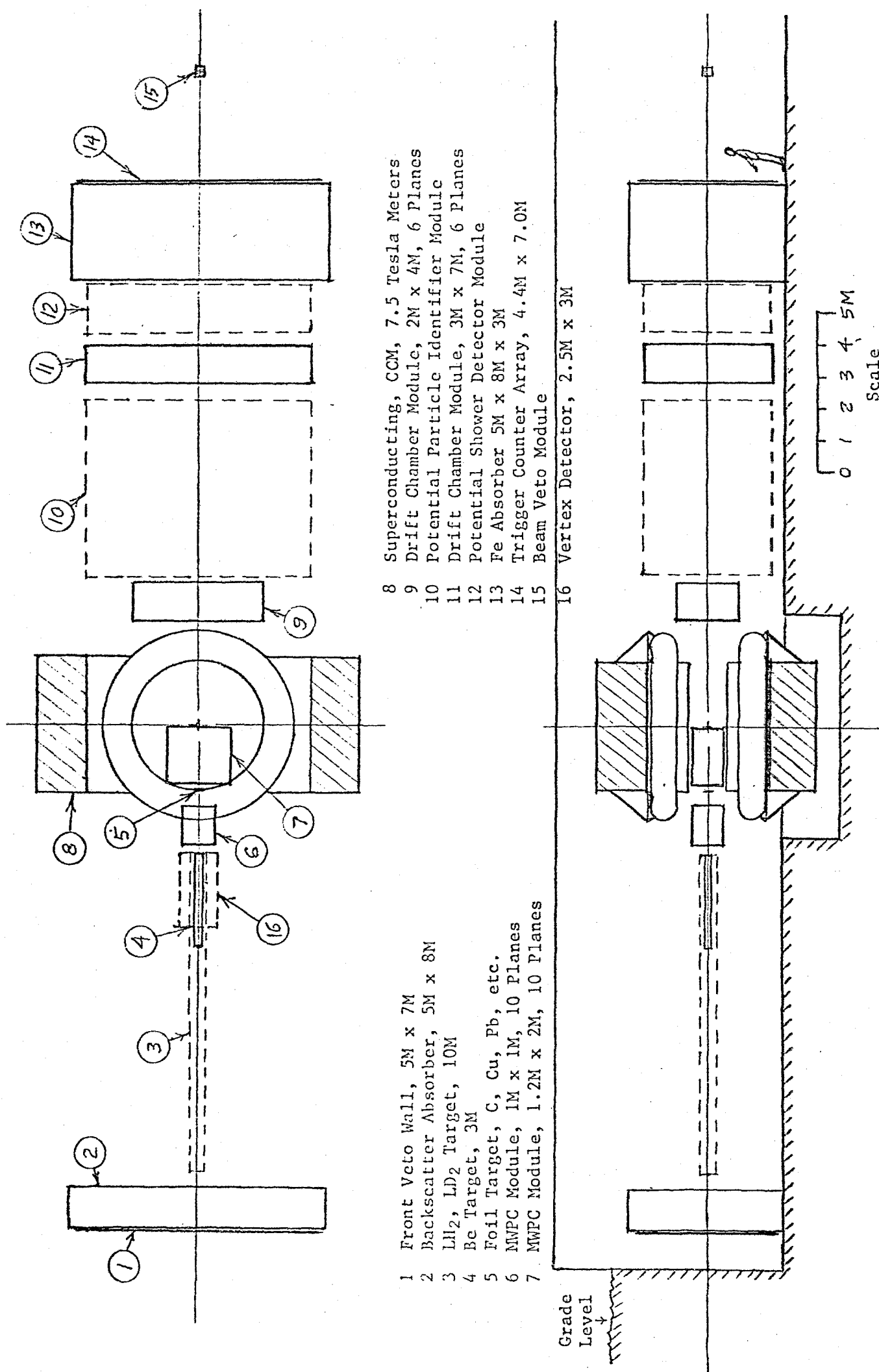


FIG. 7 (Ref. 19)



- 8 Superconducting, CCM, 7.5 Tesla Meters
- 9 Drift Chamber Module, 2M x 4M, 6 Planes
- 10 Potential Particle Identifier Module
- 11 Drift Chamber Module, 3M x 7M, 6 Planes
- 12 Potential Shower Detector Module
- 13 Fe Absorber 5M x 8M x 3M
- 14 Trigger Counter Array, 4.4M x 7.0M
- 15 Beam Veto Module
- 16 Vertex Detector, 2.5M x 3M

- 1 Front Veto Wall, 5M x 7M
- 2 Backscatter Absorber, 5M x 8M
- 3 LiH_2 , LD_2 Target, 10M
- 4 Be Target, 3M
- 5 Foil Target, C, Cu, Pb, etc.
- 6 MWPC Module, 1M x 1M, 10 Planes
- 7 MWPC Module, 1.2M x 2M, 10 Planes

Figure 8 CCM Spectrometer - Phases I, III

FIG 9a

ACCEPTANCE
 3 METER BE
 E = 600 GeV

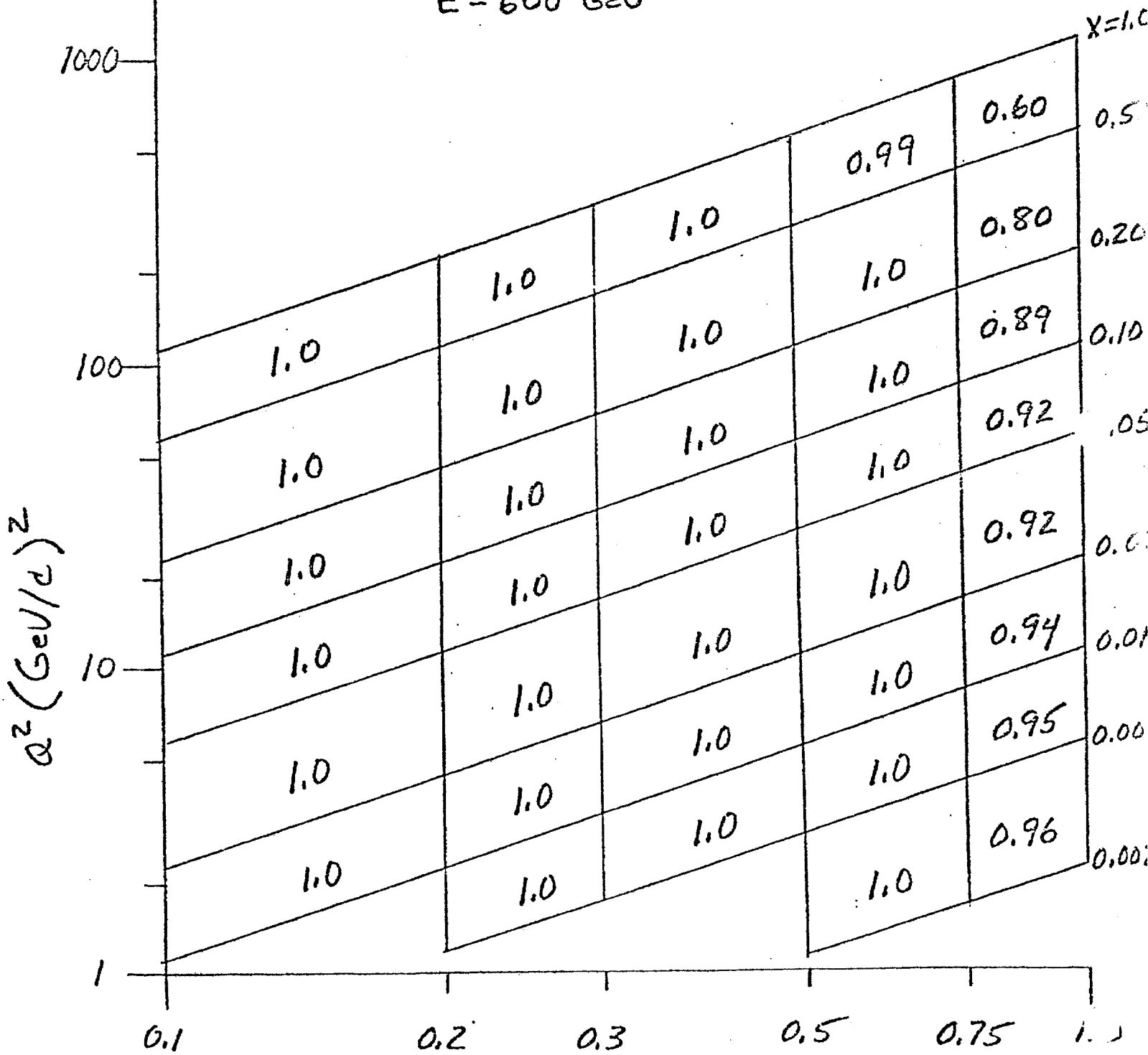


FIG 9b

ACCEPTANCE
 10 METER Hz
 E = 600 GeV

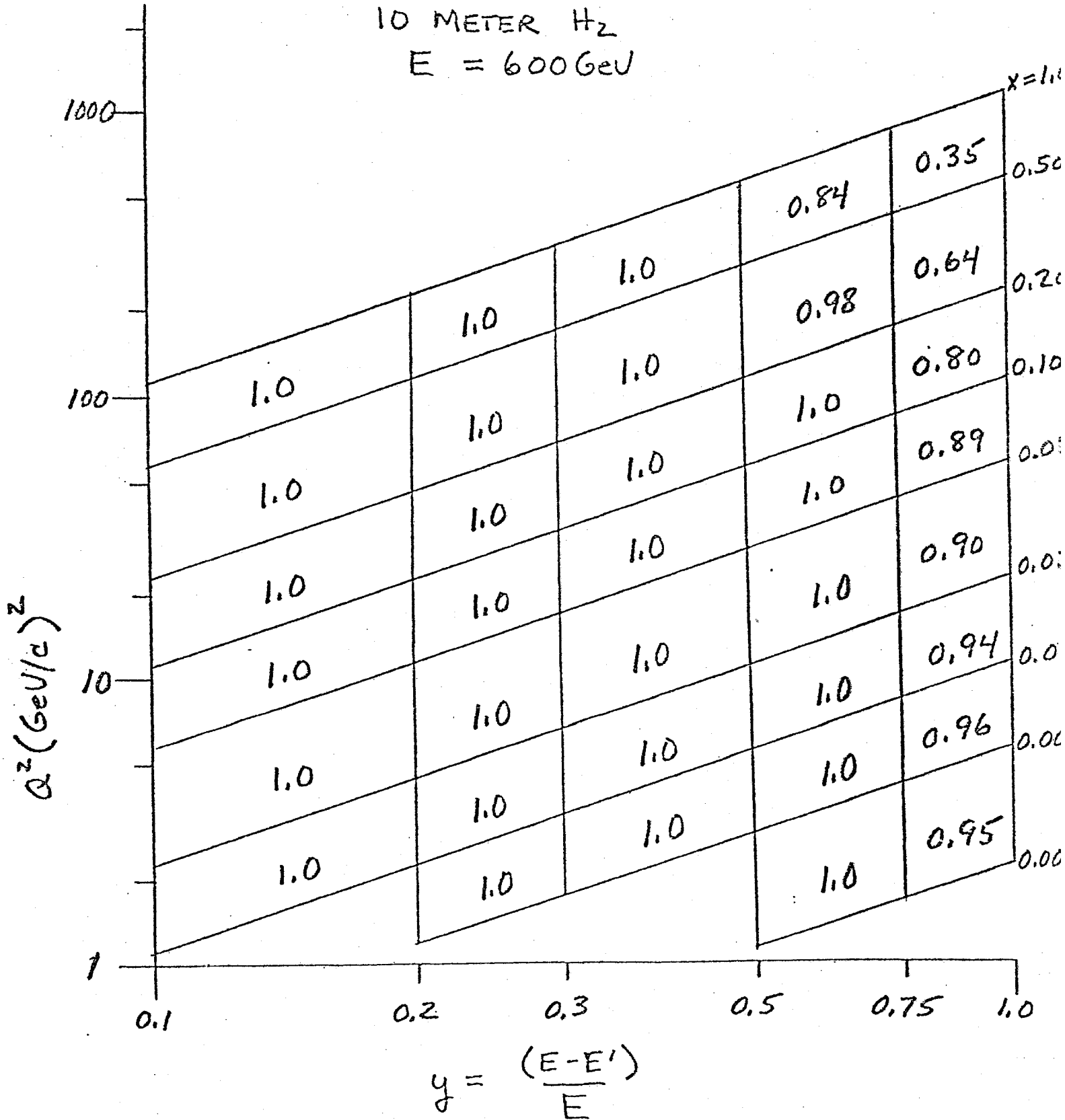
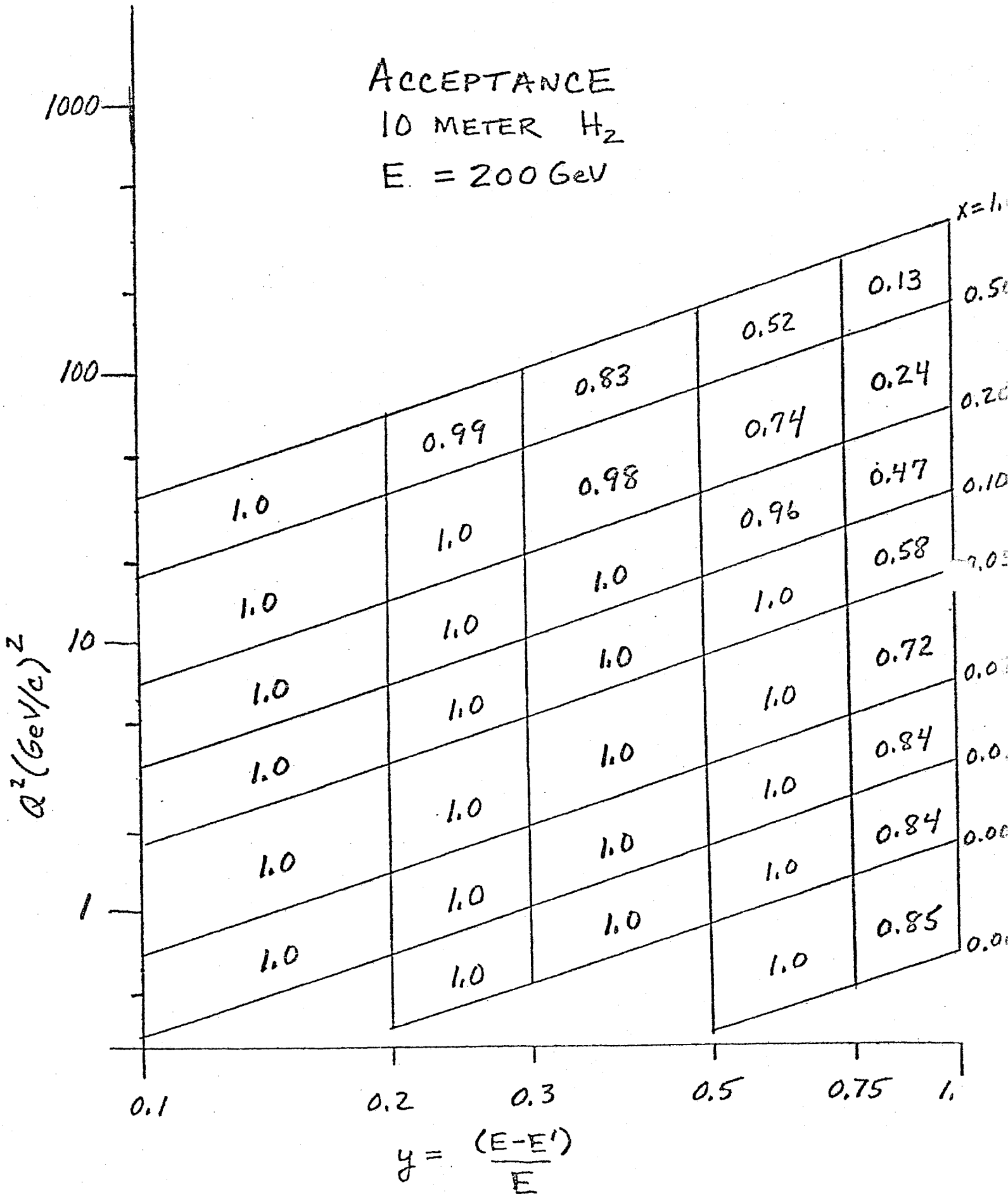


FIG 9c

ACCEPTANCE
 10 METER H₂
 E = 200 GeV



RADIAL VARIATION OF CYCLOTRON MAGNET FIELD

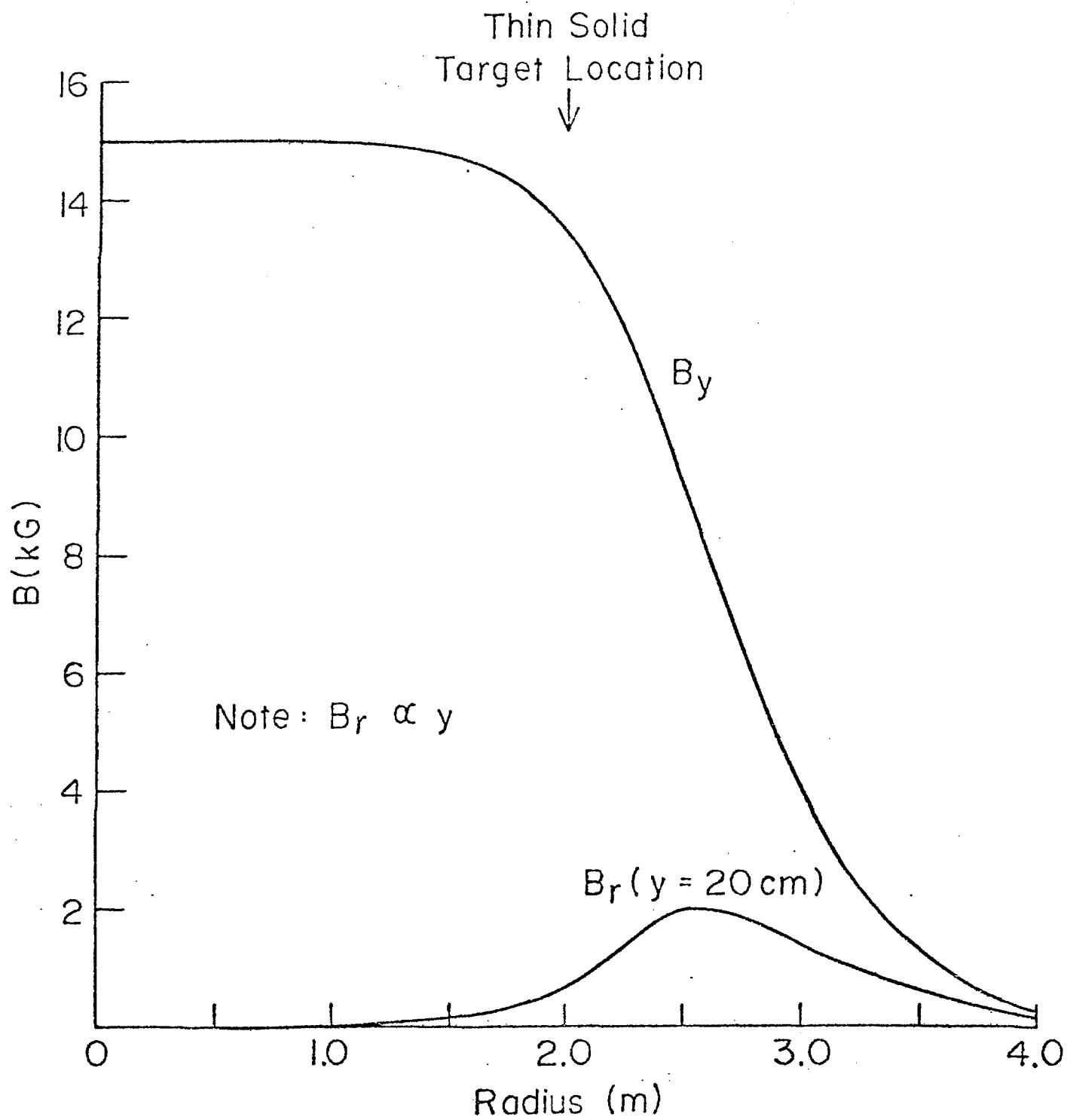


FIG. 10

VERTEX MAGNET - END AND SIDE VIEWS

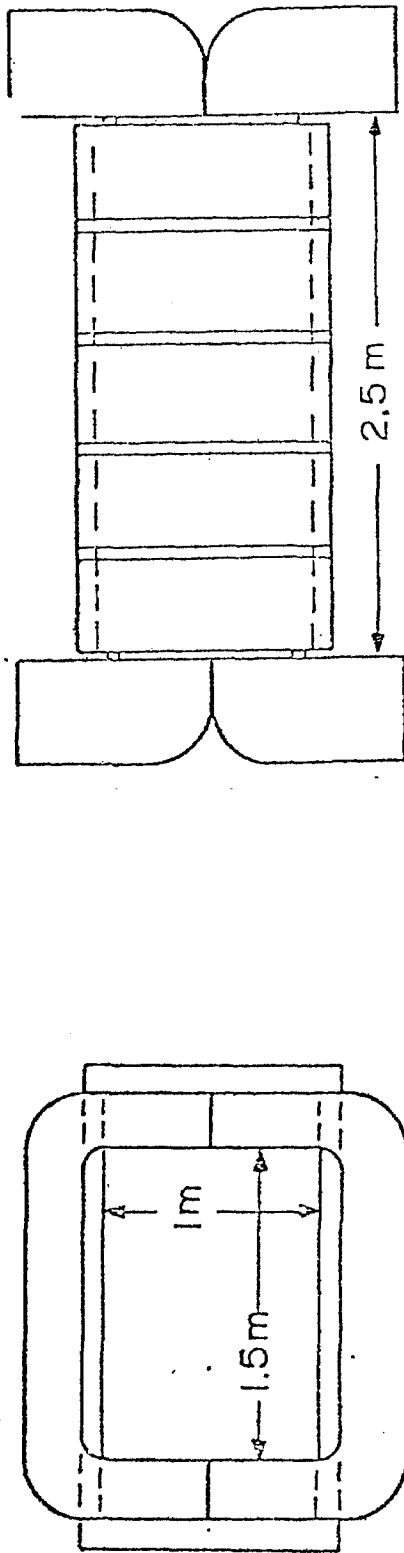


FIG. 11a

VERTEX MAGNET - HYDROGEN TARGET

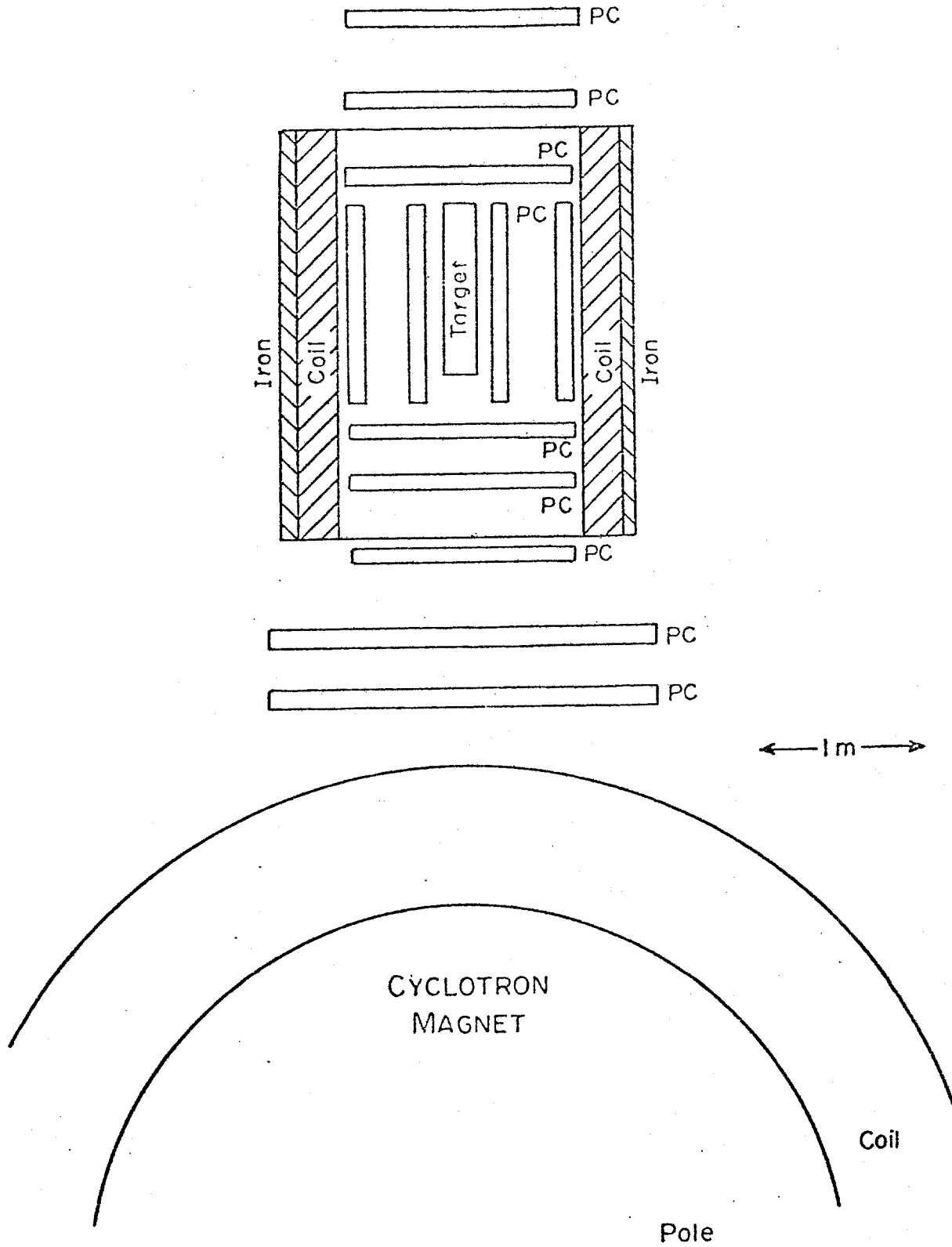


FIG. 11b

VERTEX MAGNET - TWO SOLID TARGETS

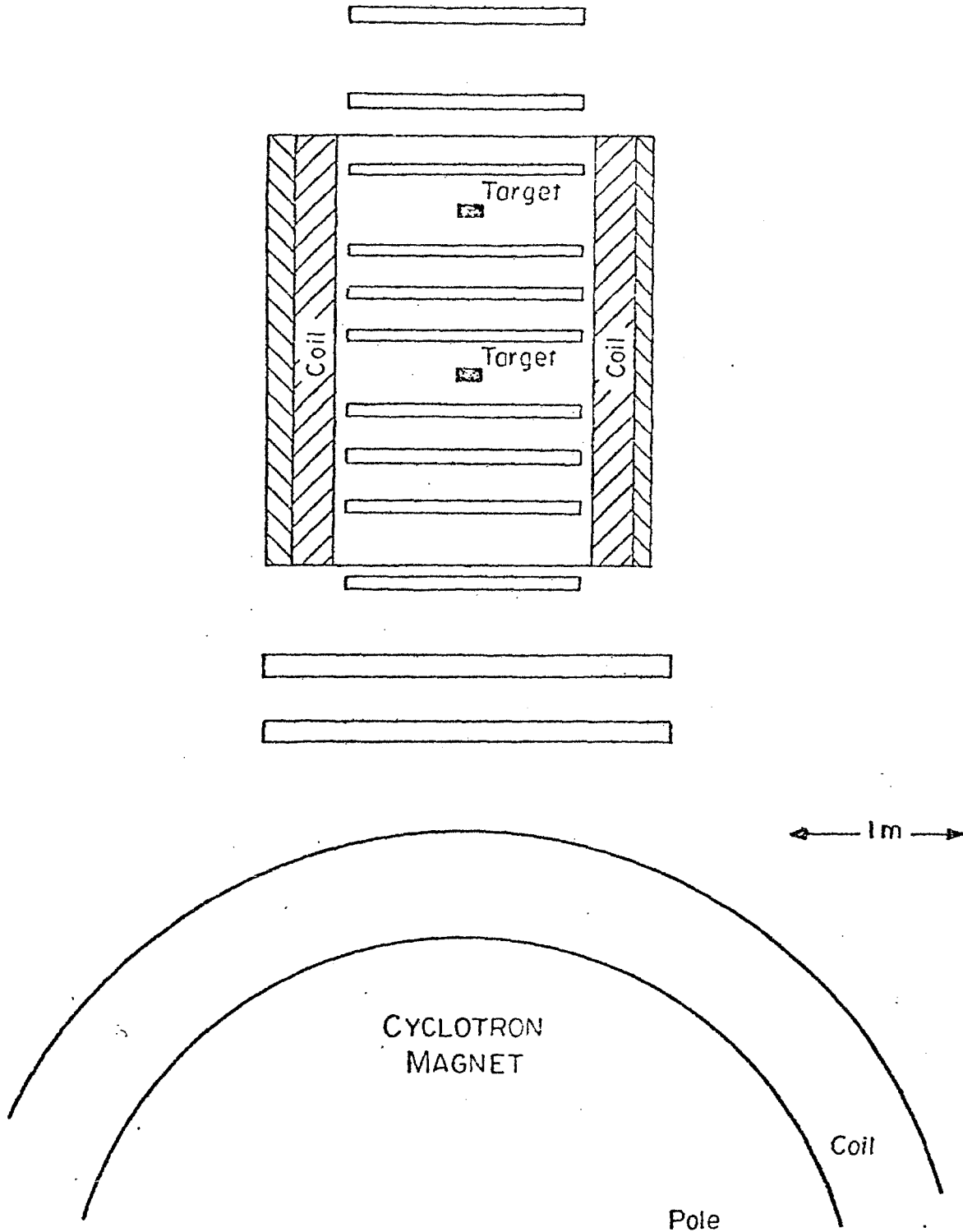


FIG. 11c